Identification of A Coprinellus Strain and Its Application in Eucommia ulmoides Gum Extraction by Fermenting Leaves

Yu Yang (932184133@qq.com)
Guizhou University https://orcid.org/0000-0002-9783-1438

Research Article

Keywords: Coprinellus disseminatus, identification, solid fermentation, gutta-percha, FTIR

Posted Date: January 23rd, 2023

DOI: https://doi.org/10.21203/rs.3.rs-2437298/v1

Version of Record: A version of this preprint was published at Biotechnology Letters on May 27th, 2023.
See the published version at https://doi.org/10.1007/s10529-023-03396-6.

Abstract

White rot fungi are a kind of filamentous fungi which can degrade lignin, hemicellulose and cellulose effectively. In this study, a wild macrofungi collected from Pingba Town, Bijie City of China was identified as *Coprinellus disseminatus* (fruiting body) based on morphological and molecular identification. The hyphae of *C. disseminatus* were pure-cultured to form *Coprinus disseminatus* (mycelium). The mycelium cultured in the medium with glucose as carbon source represented round in shape with gray color and the mycelia in the center were densely with loose margin, while the mycelium grew in the medium with xylan as carbon source appeared nearly round shape with white color and the mycelia were relatively dense from the center to the margin during all growth stages. The results of *C. disseminatus* mycelium culture under condition of xylan as sole carbon showed that the xylanase (XLE) activity and cellulase (CLE) activity were significantly higher than that of the control group (carbon-free), indicating that xylan could induce the high expression of XLE and CLE. Meanwhile, combined the mycelium culture with the determination of enzyme activity, the medium contained xylan as sole carbon was selected as the initial nutrient slution for fermentation of *Eucommia ulmoides* leaves in the following experiments. Further, the activities of tissue degradation-related enzymes including XLE, CLE, acetyl xylanesterase (AXE) and α-L-arabinofuran glycosidase (α-L-AF) were determined after fermenting Eucommia ulmoides leaves by inoculating *C. disseminatus* mycelium. The results showed that the activities of XLE, CLE, AXE and α-L-AF reached the maximum at 5 d after inoculation, which were 777.606 ± 4.248 $U \cdot mL^{-1}$, 9.594 ± 0.008 $U \cdot mL^{-1}$, 4.567 ± 0.026 $U \cdot mL^{-1}$ and 3.497 ± 0.10 $U \cdot mL^{-1}$ respectively. The results showed that xylan could be used as a potential carbon source for *E. ulmoides* leaf fermentation. At this moment, the activities of XLE and CLE in mycelium cultured in Glu-contained medium were 815.074 ± 7.102 $U \cdot mL^{-1}$ and 9.704 ± 0.030 $U \cdot mL^{-1}$ respectively, and the former was significantly higher than that of mycelium grew in Xyl-contained medium while the latter was equivalent to CLE activity of mycelium in xylan medium. Also, the activities of AXE and α-L-AF both reached the maximum in *C. disseminatus* mycelium cultured in glucose medium, which demonstrated the glucose could be optimal carbon source for the fermentation of *E. ulmoides* leaves with *C. disseminatus*. By comparing the yield of gutta-percha under different fermentation treatments, the extraction yield of gutta-percha were 2.156 ± 0.031% and 2.142 ± 0.044% at 7 d and 14 d after fermentation with mycelium supplemented xylan as carbon source, which were significantly higher than other groups. This study provides a theoretical reference for the preparation of gutta-percha by large-scale fermentation of *E. ulmoides* leaves with *C. disseminatus*.

Introduction

Macrofungi are eukaryotes with fruiting body and widely distributed in nature, and part of them are favored by people because of their high nutritional and economic value (Sridhar et al. 2019). However, their growth is highly influenced by environmental conditions, e.g., temperature, humidity and light, etc, resulting in morphological diversification (Song et al. 2018). Even macrofungi of the same species have great morphological differences under different conditions. More recently, Tuo et al. (2022) and Undan et al. (2016) reported the molecular identification based on amplification and sequencing of conserved

regions is a stable and reliable technique for classifying the macrofungi with same morphological characteristics. And, the most commonly used regions for macrofungal identification includes the internal transcribed spacer (ITS), ribosomal large subunit rDNA (LSU) and simple sequence repeats (SSR) (Appiah et al. 2017), and the first two have been frequently used for classification and identification among different fungal species (Mešić et al. 2020). Krishna et al. (2015) identified 10 samples as *Agaricus campestris* from collected 50 macrofungi by a combination of morphological and molecular identification. Zhang et al. (2015) investigated the relationship between *Tricholoma mongolicum* and its related species based on ITS analysis, and these closely related species were successfully distinguished. Accurate identification and classification of macrofungi provide theoretical guarantee for better utilization and exploitation of macrofungal resources. Besides its important value in agriculture, the vital function of macrofungi in industry and medicine has been extensively explored in recent years (Mckelvey et al. 2017; Andlar et al. 2018). Soccol et al. (2017) reported the macrofungal fermentation had been involved in many fields including pharmacy, textile, food industry and other fields, and the straw of many crops (e.g., oats, maize, wheat, etc) could be used as substrate for macrofungal fermentation (Camelini et al. 2013), which effectively realized the higher value application of waste.

Eucommia ulmoides (also called 'Duzhong') is an important medicinal and colloidal plant in China (Zeng et al. 2018; Healey et al. 2015). Duzhong has the functions of strengthening muscles and bones and curing lumbar spine pain according to ancient book '**Shennong's Herbal Classic of Materia Medica**'. Besides phamaceutical purposes, the *E. ulmoides* gum (known as gutta-percha) is also an important raw material for the development of a variety of new materials in medical, communicational and military field (Wei et al. 2021) due to unique rubber and plastic duality. Although gutta-percha has very important application value, gutta-percha extraction is costly and difficult due to the limitation of its synthesis site (She et al. 2019). At present, physical and chemical methods are mainly adopted for gutta-percha extraction (Wang et al. 2021; Zhou et al. 2018), and these methods not only destroy the structure of gutta-percha to a certain extent but caused seriously environmental pollution during the extraction process (Liu et al. 2022). Recently, solid fermentation mediated by microorganism is effective to destroy the cell wall structure of plant tissues, so as to ensure the integrity and yield of secondary metabolites (Healey et al. 2015). Considering the important value of *E. ulmoides*, fungal fermentation using *E. ulmoides* tissue as substrate has been extensively studied. Xu et al. (2018) conducted fermentation of *E. ulmoides* leaves with *Cordyceps militaris*, which significantly increased the yield of cordycepin by 60.44%, Wu et al. (2021) improved the extraction rate of total flavonoids and gutta-percha by pretreating *E. ulmoides* leaves with combination of ultrasonic microwave and fungi. Qian et al. (2020) reported a white rot fungus, *Inonotus obliquus*, had preferably degraded effect on *E. ulmoides* leaves with higher lignocellulase activity, while Zhu et al. (2018) improved significantly the gutta-percha yield by fermenting pericarp of *E. ulmoides* samara with *Aspergillus* D-5, and the removal rate of cellulose substances reached 86.43%. In this study, another saprophytic fungi called BJ-1 collected in the field were used to ferment *E. ulmoides* leaves. After identification by molecular method, the activities of these enzymes (e.g., CLE, XLE, AXE and α-L-AF) involved in degradation of plant tissue were determined, and the fermented extracts were further

identified by FTIR, which provided a theoretical basis for the large-scale preparation of gutta-percha by the fermentation of *E. ulmoides* leaves with *Coprinellus* strain.

Materials And Methods

Materials

The wild macrofungi grew in decaying leaves and wood in evergreen deciduous broadleaved forest dominated by *Quercus linna* were collected. The leaves used for fermentation from *E. ulmoides* 'Huazhong 6', which were collected from the '**Eucommia Resource Nursery of Institute**' of Agro-Bioengineering of Guizhou University. Cellulase Test Kit (Code No. A138-1-1) was purchased from Nanjing Jiancheng Bioengineering Institute (China), and α-L-arabinofuran glycosidase Test Kit (Code No. BC4765) were purchased from Beijing Solarbio Science & Technology Co., Ltd (China). The 2-hydroxy-3, 5-dinitrobenzoic acid (DNS, Cas No. 609-99-4), D-(+)-Xylose (Cas No. 58-86-6), xylan (poly-β-D-xylopyranose (1→4) Cas No. 9014-63-5), D-(+)-glucose (Cas No. 50-99-7), dimethyl sulfoxide (DMSO, Cas No. 67-68-5) and p-nitrophenol acetate (Cas No. 830-03-5) were purchased from Sigma-Aldrich (Merck, USA). The petroleum ether (AR) and absolute ethanol (AR) were purchased from Tianjin Kemiou Chemical Reagent Co., Ltd (China).

Methods

Field Survey and Macrofungi Collection

According to the method of Senanayake et al. (2020), field investigation of macrofungi were carried out in Pingba Town, Jinsha County, Bijie City, Guizhou Province of China (105°47'—106°44' E, 27°07'—27°46' N) from May to September, 2021. The altitude sampling site is 739-1460 m and the average annual temperature is about 15℃, and the forest coverage rate is 56.2% and the average annual rainfall is 1030-1100 mm. According to difference of vegetation types and terrain, the wild macrofungi grew in decaying branches and leaves on the ground and in live tree trunks on different slopes were investigated. The collected wild macrofungi were photographed, recorded and stored, and the fruiting bodies were brought back to the laboratory for subsequent research.

Fungal Identification and Pure Culture of Mycelium

Based on the method reported by Zhou (2009), the morphological characteristics (e.g. pileus, stipitipellis, lamella and teleblem, etc) of the collected wild macrofungi (fruiting body) were observed and identified. According to the method of Passari et al. (2016), the base of the fruiting body stalk was removed and placed in the inoculating chamber. After surface sterilization with 75% alcohol, a flame-sterilized scalpel was used to make a longitudinal cut in the middle of fruiting body stalk and then the fruiting body were broken off by hand and five small squares were cut at the junction of the pileus and stipitipellis of macrofungi with an inoculating shovel. Then, a small piece of tissue was selected and quickly transferred to the beveled PDA medium (20 $g \cdot L^{-1}$ glucose, 2 $g \cdot L^{-1}$ peptone, 2 $g \cdot L^{-1}$ yeast extract, 0.5 $g \cdot L^{-1}$

$MgSO_4 \cdot 7H_2O$ 0.46 g·L^{-1} KH_2PO_4 20 g·L^{-1} agar powder, natural pH) for culture at 28 ± 2℃, and the mycelium formed from unpolluted tissue block. After 3 to 5 secondary cultures, the pure mycelium were acquired for subsequent studies. Total genomic DNA of pure mycelium was extracted according to the method of Huang et al. (2018) and Wu (2015) (with minor modifications), and the primer ITS1/ITS4 and LROR/LR5 were used to amplify conserved regions including internal transcribed spacer (ITS) and ribosome large subunit DNA (LSU) according to the method reported by Febriansyah et al. (2018) respectively. The primer sequence for ITS and LUS amplification were shown in Table **1**. Finally, the amplified products were sequenced by Shengong Bioengineering (Shanghai) Co., LTD. Blast alignment was performed according to the method of Roy et al. (2018) and the phylogenetic tree was constructed by MEGA 7.

Table **1**

Effects of Different Carbon Sources on Mycelium Growth

According to the method of Liu et al. (2021), the purified mycelium was inoculated on the medium (2 g·L^{-1} peptone, 2 g·L^{-1} yeast extract, 0.5 g·L^{-1} $MgSO_4 \cdot 7H_2O$, 0.46 g·L^{-1} KH_2PO_4, 20 g·L^{-1} agar powder, natural pH) supplemented with glucose or xylan as sole carbon source respectively, with the medium without carbon source as control. Each group was independently repeated for 3 times, and the morphology of hypha and mycelium of macrofungi was observed and photographed. Meanwhile, mycelium growth amount was calculated according to the following Formula **1**.

Hypha growth amount (HGA) = (mycelium diameter - inoculum diameter) /2 Formula **1**

Effects of Xylan Carbon Source on Cellulase and Xylanase Activities

To investigated the effects of xylan carbon source on CLE and XLE activities, the depurative mycelium block (d=1 cm) was taken out from solid medium with aseptic puncher and transferred the mycelium to liquid medium (2 g·L^{-1} peptone, 2 g·L^{-1} yeast extract, 0.5 g·L^{-1} $MgSO_4 \cdot 7H_2O$ 0.46 g·L^{-1} KH_2PO_4, natural pH) contained xylan, with no-carbon source medium as control. At different days after shaking culture with 180 r·min^{-1} under 28℃, an equivalent amount of pure culture was taken out to measure XLE activity according to the method reported by Meng et al. (2021) and CLE activity was measured according to the instruction of Cellulase Test Kit (Nanjing Jiancheng Bioengineering Institute). Each treatment was repeated 3 times.

Effects of Xylan Carbon Sources on Activities of Tissue Degradation-correlated Enzymes during Fermentation

To further survey the decomposability of *C. disseminatus* mycelium to leaf tissue, the purified mycelium was inoculated into a triangular flask containing sterilized *Eucommia* leaves for solid fermentation according to the method of Qian et al. (2020). The freshly picked *E. ulmoides* leaves were dried at 60℃ to a constant weight, then were gently rubbed and crushed for fermentation. Meanwhile, an equivalent

amount of liquid medium was added to the leaves solid matrix as the nutrient for mycelial fermentation at initial stage. The supplemental liquid medium included carbon-free medium (CFM) 2 $g \cdot L^{-1}$ peptone, 2 $g \cdot L^{-1}$ yeast extract, 0.5 $g \cdot L^{-1}$ $MgSO_4 \cdot 7H_2O$, 0.46 $g \cdot L^{-1}$ KH_2PO_4, natural pH), xylan-carbon medium (XCM) (20 $g \cdot L^{-1}$ xylan, 2 $g \cdot L^{-1}$ peptone, 2 $g \cdot L^{-1}$ yeast extract, 0.5 $g \cdot L^{-1}$ $MgSO_4 \cdot 7H_2O$, 0.46 $g \cdot L^{-1}$ $KH_2PO_4$20 $g \cdot L^{-1}$ agar powder, natural pH), with supplemental sterile water as control. Weighed exactly 5.0 g crushed *E. ulmoides* leaves to clean culture flask and mixed with supplemental liquid medium according to a ratio of 1 leaves : 1 liquid medium, and an equivalent amount (~1 cm^2 mycelium block) was inoculated into leaves matrix above for continuous fermentation at 28℃ under dark conditions. At different days (3, 5 and 7 d) after fermentation, the activities of XLE and CLE were determined according to description above, and the activities of AXE and α-L-AF were determined according to the method of Krastanova et al. (2005) and the operation of α-L-arabinofuran glycosidase Test Kit (Beijing Solarbio Science & Technology Co., Ltd) respectively.

Effects of Different Conditions on Extraction Rate of Gutta-percha

At 7 d and 14 d after fermentation, the fermented *E. ulmoides* leaves were dried at 60℃ to constant weight, and gutta-percha extraction was conducted according to the method reported by Wei et al. (2021) and Yuan et al. (2021) (with minor modifications). The dried *E. ulmoides* leaves and petroleum ether were mixed according to a solid-liquid ratio of 1 : 20, and the gutta-percha was extracted on a Soxhlet extractor at 90℃ for 24 h. After that, the extract was placed at a low temperature of -20℃ for 3 h to precipitate the gutta-percha. After natural drying of precipitation, the dried precipitates was refined *E. ulmoides* gum, and the yield of refined gum was calculated according to Formula **2**.

Refined gum yield (RGY) = (Dry mass of refined gutta-percha from extraction/total dry mass of sample) × 100% Formula **2**

Determination of Gutta-percha Based on Fourier Transform Infrared Spectroscopy

Accurately weighed 10 mg of gutta-percha dried to constant weight for weighed for tablet pressing according to the method of Cui et al. (2022). The processed tablet samples were placed into a Fourier Transform Infrared Spectroscopy (FTIR) (spotlight 200) for scanning identification, comparison and analysis. The spectral region ranged from 4000-400 cm^{-1}, and the maximum resolution was 2.0 cm^{-1}. Addtionally, the detector was a DTGS detector and the light source is air cooled ceramic light source.

Data Analysis and Data Processing

IBM SPSS Statistics 18.0 were used for data analysis and GraphPad Prism 9.0 were used for mapping respectively.

Results

Description of Habitat and Fruiting Body morphology of Collected Macrofungus

Based on the results of field survey, the collected macrofungus principally grew in scattered on dead branches and rotten leaves on ground in evergreen deciduous coniferous/broad-leaved mixed forests (Fig. **1A**). Further, identification based on morphological characteristcs of the vegetation in habitat, the plants in the mixed forest mainly included *Quercus mongolica* belonged to family Fagaceae, *Maclura pubescens* belonged to family Moraceae and *Pinus massoniana* belonged to family Pinaceae, etc. In addition, morphological observation of fruiting body showed it was a kind of macrofungus with medium size, and the fruiting body as a whole was white to off-white. The pileus manifested as an inverted bell-shape with several small black spots on it, and the center of the pileus bulged upward with a diameter of about 1.5-2 cm. The mediotrastum was thin and sparse and the stipitipellis was slender and hollow with an average length of 5 cm. According to the collection number, the macrofungus was labeled as 20210527JSYY-06 (Fig. **1B—E**). To facilitate the description on subsequent research, it was named BJ-1.

Fig. **1**

Molecular Identification and Phylogenetic Analysis of BJ-1

Total DNA of pure mycelium of BJ-1 was extracted, and two conserved regions (ITS and LSU) were amplified with specific primers ITS1/ITS4 for ITS and LROR/LR5 for LSU, and a clear single band between 500 to 750 bp and 750 to 1000 bp (Figure **S1**) were obtained respectively. The amplified products were sequenced by Shengong Bioengineering Co., LTD, and the sequence of conserved regions was obtained. Alignment result based on ITS sequence showed that the conserved region (accession No. OP735466) of BJ-1 was highly homologous (99.69%) with the sequence (accession No. KY243924.1) of *Coprinellus disseminatus* (isolated by Prabhu, India), while LSU-conserved region (accession No. OP735472) of BJ-1 was also highly similar to conserved region of *C. disseminatus* A2S6-11 (accession No. KJ780770.1). Based on the alignment results of the two conserved regions above, it cloud speculate the BJ-1 belonged to a specie of *C. disseminatus* according to judging principle reported by Altaef et al., (2021). Clustering results based on ITS sequence by MEGA 7.0 showed that the ITS-conserved region of BJ-1 was 96% genetic relationship with *C. disseminatus* (accession No. KJ832042.1) (Fig. **2**). Meanwhile, the BJ-1 had been sent to Guangdong Microbial Culture Collection Center (GDMCC) (http://www.gdmcc.net) for preservation and the number of culture preservation was 5.797.

Figure **S1**

Fig. **2**

Morphological Comparison of Mycelium Grew in Medium with Different Carbon Sources

Generally, the mycelium of BJ-1 grew on the medium appeared gray or grayish white in color, and the edges of mycelium were regular or irregular in appearance. The amount of mycelium increased with the increase of culture time. The mycelium on the medium with xylan as carbon source was regularly round in shape, and mycelium was white and dense. On the contrary, the mycelium cultured on medium with glucose as carbon source showed a nearly circular shape with a dense center and loose edge, and the

mycelium was grayish white in color. Additionally, the mycelium on the carbon-free medium was irregular in shape and the mycelium were loose and gray from center to the edge (Fig. **3**). Microscopic observation showed that the hypha of BJ-1 cultured on carbon-free medium was slender and septate, with few or no branches. However, the hypha grew on glucose or xylan-contained medium was almost nonseptate with some branches in the former and without branches (Fig. **4**). The results above indicated that there was a significant effect of carbon source on morphology of BJ-1 hyphae and xylan as carbon source could increase mycelium density, which was similar to the culturing results of *Piptoporus soloniensis* conducted by Kanwal et al. (2012). Additionally, it could be seen from Figure **S2**, the mycelium of BJ-1 showed a slow upward trend on the carbon-free, glucose- and xylan-contained medium with the increase of culture time.

Fig. **3**

Fig. **4**

Figure **S2**

Analysis of CLE and XLE Activities of BJ-1 Mycelium on Medium with Xylan Carbon Sources

Based on the early reports conducted by Singh et al. (2009), *C. disseminatus* possessed high XLE and low CLE activity during growth and metabolism, which had been used to bleach pulp in consideration of strong lignin degradation ability mediated by XLE (Singh et al. 2011). Yan et al. (2022) believed that the activity level of these physiological metabolism-related enzymes reflected the growth state of mycelium to a certain extent. Synchronously, the degradation of cellulose and lignin in plant cell wall depended on the interaction of these enzymes (Andlar et al. 2018). The determination of XLE and CLE activity in mycelium showed the activities of both enzymes increased firstly and then decreased to be stable with the culture times. At 6 d, the XLE activity of mycelium reached the maximum (49.434 ± 0.933 $U{\cdot}mL^{-1}$), which was significantly higher than that of carbon-free group (45.360 ± 0.614 $U{\cdot}mL^{-1}$) (Fig. 5A).) Howecver, the CLE activity of mycelium achieved the maximum (8.101 ± 0.048 $U{\cdot}mL^{-1}$) at 5 d, which was significantly higher than that of carbon-free group (7.156 ± 0.086 $U{\cdot}mL^{-1}$) (Fig. **5B**). These studies above showed that the additional supplement with xylan as carbon sources could dramatically improve the activities of XLE and CLE in mycelium of BJ-1.

Fig. **5**

Activities Comparison of Tissue Degradation-correlated Enzymes in Mycelium during Fermentation

Further, the activities of tissue degradation-correlated enzymes (e.g. AXE and α-L-AF) besides XLE and CLE were also determined. At 7 d after inoculation with BJ-1, the mycelium of BJ-1 overgrew the entire surface of *Eucommia* leaves no matter what kind of the fermentation conditions (Fig. **6**), which suggested the BJ-1 could grow well in *E. ulmoides* leaves-based matrix. At 3 d after inoculation with BJ-1, the activities of XLE, CLE, AXE and α-L-AF were relatively low, which it was speculated that the mycelium

might be in the growth adaptation period with low growth rate. However, the XLE activity reached the maximum with 756.754 ± 4.783 U·mL^{-1} U·mL^{-1} in xylan-contained group, followed by carbon-free group (708.319 ± 2.758 U·mL^{-1}), and the minimum XLE activity was found in medium-free group (667.489 ± 10.202 U·mL^{-1}). And, the CLE activity of mycelium decreased in sequence in the following groups including xylan-contained group, carbon-free group and medium-free. Additionally, at 5 d after inoculation, the maximum activity of AXE and α-L-AF were found in xylan-contained group, which were 4.657 ± 0.036 U·mL-1 and 3.497 ± 0.140 U·mL-1 respectively, followed by carbon-free group (Fig. 7). The variation trend of CLE and XLE activity during fermentation were consistent with that in mycelium culture with different culture conditions. The above studies showed that xylan had a significantly promoting effect on the the activities of the CLE, XLE, AXE and α-L-AF, and the supplement of xylan had a certain difference in the improvement of the activities of the four enzymes.

Fig. **6**

Fig. **7**

Effects of Initial Supply of Carbon Sources on Gutta-percha Yield during Fermentation

All *E. ulmoides* leaves after fermentation by inoculating BJ-1 manifested as slightly dark brown in color while the unfermented leaves appeared brown (Fig. **8**), and the organization structure of fermented leaves was loose and fluffy compared with these unfermented *E. ulmoides* leaves, which implied the metabolic activity of BJ-1 mycelium degraded the tissue structure of *E. ulmoides* leaves and the tissue-decomposed ability was supposed to be a joint action of multiple enzymes. Wu et al. (2021) reported the pretreatment of *E. ulmoides* leaves with the combination of ultrasonic, microwave and fungus could improve the yield of total flavonoids and gutta-percha by decomposing structure of plant tissue. And, the determined results of gutta-percha yield showed that extraction rate of crude and refined gutta-percha in the medium-free group (only sterile water without BJ-1) were the lowest at 7 d, being 23.82% and 1.62% respectively, followed by the water-substitute group (carbon-free medium replaced by sterile water with BJ-1), being 26.51% and 1.68% respectively. The above results indicated that not only BJ-1 was necessary to improve the extraction yield of gutta-percha, but the carbon-free nutrient components were also important to enhance the activity of BJ-1 and improve the gutta-percha yield, which the result was similar to the study of Qian et al. (2020). In addition, the selection of different carbon sources will indirectly affect the XLE and hemicellulase activities of BJ-1 mycelium, resulting in different degrees of degradation of *E. ulmoides* leaves, which was ultimately reflected in the difference in the extraction rate of gutta-percha (Jordan et al. 2012; Sipos et al. 2010).

Gutta-percha Identification Based on FTIR Analysis

To further confirm whether the extracted product being gutta-percha or not, the FTIR analysis was executed. The results showed that the absorption peaks of extract obtained by fermentation were all in the range of 400~4000 cm^{-1}. Among them, the absorption peak at 972-1660 cm^{-1} was the unsaturated hydrocarbon absorption peak formed after stretching vibration of C=C double bond, while the absorption

peak at 2700-3000 cm^{-1} was the saturated hydrocarbon peak of C-H single bond. And, the strong absorption peak at 3400 cm^{-1} showed the presence of hydroxyl group (-OH) (Figure **S3** and Figure **S4**). This result was consistent with the identification results of gutta-percha by infrared spectroscopy reported by Yu et al. (2019) and Cui et al. (2022), which demonstrated the extract from *Eucommia* leaves by fermenting was exactly gutta-percha (*E. ulmoides* gum), and the structure of gutta-percha was intact.

Table **2**

Fig. **8**

Figure **S3**

Figure **S4**

Discussion

Macrofungus is a kind of saprophytic microorganism which takes plant dead leaves as nutrient substrate, and it plays an important role in degrading plant residues and promoting ecological cycle (AlessiaBani et al. 2018). In this paper, a strain of *Coprinellus* was collected during the investigation of macrofungi in Bijie city of Guizhou province, China. The survey results showed that the strain grew in decaying plant remains consisting of dead leaves and branches, and the latter provided rich nutrients for growth of strain (Alanbagi et al. 2021). The results based on morphological comparison and molecular identification (ITS and LSU) indicated that the strain was eventually identified as *C. disseminatus* of *Pseudocoprinus* in Psathyrellaceae family, and it was designated as BJ-1. The mycelium culture of BJ-1 showed that the xylan induced a denser mycelium compared with glucose, which inferred xylan as an unfavourable selection pressure promoted the increase of mycelium. Xylan is a kind of heterologous polysaccharide in plant cell wall, accounting for about 15%~35% of the dry weight of plant cells, which is the main component of plant hemicellulose and a kind of complex five-carbon-based polysaccharide (Terrett et al. 2019). Therefore, it is reliable and effective reagent for screening the microorganisms that could utilize xylan as the sole carbon source for growth. Well growing status of BJ on xylan-contained medium implied the strain could effectively utilize xylan for growth, which it was similar to the culture results of *Cordyceps militaris* mycelia (Dang et al. 2018). The results of enzyme activity showed that there was significant difference in activities of CLE and XLE of BJ-1 on medium supplemented with different carbon source. As a whole, the XLE activity of mycelium on glucose-contained medium was significantly higher than that on xylan-contained one, but both were significantly higher than that on carbon-free medium, which suggested that 1) the supplement of carbon source could improve the XLE activity; 2) the glucose and xylan promoted and inhibited the XLE activity respectively. Conversely, the CLE activity of mycelium on xylan-contained medium was significantly higher than that on glucose-contained one, which suggested the xylan promoted the CLE activity while the glucose suppressed the CLE activity. Both CLE and XLE activity showed strong dependence on carbon source, which is similar to *Lentinula edodes* mycelia cultured on different carbon sources, which displayed significant difference in

activities of CLE, XLE and endoglucanase on medium supplemented with different carbon sources (Cai et al. 2017). Xylan is the main component of plant hemicellulose, accounting for ~ 32.5% of the dry weight of plant cells, and XLE can effectively degrade xylan into xylose (Basit et al. 2019), while AXE is another important enzyme for hemicellulose degradation, which mainly hydrolyzes the 2’ and 3’ position O-acetyl groups on xylose residues in xylan (Sista et al. 2018). Besides, α-L-AF is a glycosidase capable of hydrolyzing non-reducing furanoarabinose residues of neutral sugars (e.g., arabingalactan and arabinmannan) in plant cell walls. As a result, it can promote the solubilization and degradation of pectin (Diarte et al. 2021). The activities of these enzymes including α-L-AF, XLE, CLE and XLE were determined during fermentation of *E. ulmoides* leaves showed the variation trend of CLE and XLE activity was consistent with the results of mycelium culture without *E. ulmoides* leaves. However, the activities of AXE and α-L-AF reached the maximum at 5 d after fermentation with adding xylan-contained medium to leaves. Although the glucose was the optimal carbon source for improving the XLE activity in culture of BJ-1 mycelium, xylan could increase the activities of the enzymes involved in degrading plant cell wall simultaneously during fermentation, which implied xylan could be used as the optimal carbon source for the large-scale preparation of gutta-percha by fermented *E. ulmoides* leaves with BJ-1. Meanwhile, the crude and refined gutta-percha from fermented products was calculated. The results showed that yield of crude gutta-percha extracted from mycelium-fermented *E. ulmoides* leaves supplemented xylan were 51.623 ± 9.861% and 49.728 ± 3.912% at 7 d and 14 d respectively, which were significantly higher than other groups. In addition, the yield of refined gutta-percha was significantly higher than those extracted by alkaline method (1.687 ± 0.009%), enzymatic hydrolysis method (1.160 ± 0.014%) and ultrasonic method (1.697 ± 0.015%) reported by Xie et al. (2023). The results above showed that BJ-1 could be used as the dominant strain for preparing gutta-percha on large-scale by fermentation, and the supplementation of xylan as carbon source nutrients at the initial stage of fermentation could significantly improve the ability of BJ-1 to degrade leaf tissue.

Declarations

AUTHOR CONTRIBUTIONS

Y Y : Data analysis, writing — original draft Supervision and project administration.

FUNDING

This study was funded by Key Project of Guizhou Science and Technology Plan (2019-2451).

DECLARATIONS

Conflflict of interest The authors have declared no conflflict of interests.

Ethical approval

This article does not contain any studies with animals performed by any of the authors.

References

1. Alanbagi RA, Alshuwaili FE, Stephenson SL (2019) Fungi associated with forest floor litter in northwest Arkansas. J. Fungal Biol. 9(1): 25-35
2. AlessiaBani S, Maurizio V, Luigimaria B et al (2018) The role of microbial community in the decomposition of leaf litter and deadwood. Appl soil ecol. 126(5): 75-84
3. Altaef A, Khesraji T O, Maroff MN (2021) Morphological and molecular identification of four coprinoid macrofungal species, three new records macromycota in Iraq. Plant Cell Biotechnol. and Mol. Biol. 22(37&38): 91-102
4. Andlar M, Rezić T, Marđetko N, Daniel K R, Božidar Š (2018) Lignocellulose degradation: An overview of fungi and fungal enzymes involved in lignocellulose degradation. Eng Life Sci 18(11): 768-778
5. Appiah T, Agyarem C, Luo Y (2017) Molecular identification of some Ghanaian mushrooms using internal transcribed spacer regions. Mol. Biol.$^{+}$ 6(3): 1-5
6. Basit A, Miao T, Liu JQ et al (2019) Highly efficient degradation of xylan into xylose by a single enzyme. Acs. Sustain Chem. Eng. 7(13): 11360-11368
7. Cai YL, Gong YH, Li W et al (2017) Comparative secretomic analysis of lignocellulose degradation by *Lentinula edodes* grown on microcrystalline cellulose, lignosulfonate and glucose. J. proteomics 163(23): 92-101
8. Camelini CM, Gomes A, Cardozo F et al (2013) Production of polysaccharide from *Agaricus subrufescens* Peck on solid-state fermentation. Appl. Microbiol. Biot. 97(2013): 123-133
9. Cui GQ, Liu ZZ, Wei MX et al(2018) Turpentine as an alternative solvent for the extraction of gutta-percha from *Eucommia ulmoides* barks. Ind. Crop. Prod. 121(1): 142-150
10. Dang H, Wang HQ, Lay H (2018) Effect of nutrition, vitamin, grains, and temperature on the mycelium growth and antioxidant capacity of *Cordyceps militaris* (strains AG-1 and PSJ-1). J. Radiat Res. Appl. Sc. 11(2): 130-138
11. Diarte C, Iglesias A, Romero A et al (2021) Ripening-related cell wall modifications in olive (*Olea europaea* L.) fruit: A survey of nine genotypes. Food Chem. 338(15): 127-142
12. Febriansyah E, Saskiawan I, Mang W et al (2018) Potency of growth promoting bacteria on mycelial growth of edible mushroom *Pleurotus ostreatus* and its identification based on 16S rDNA analysis. AIP Conf. Proc. 2002(1): 719-733
13. Healey AL, Lee DJ, Furtado A (2015) Efficient eucalypt cell wall deconstruction and conversion for sustainable lignocellulosic biofuels. Front. Bioeng. Biotech. 3(20): 190-206
14. Huang X, Duan N, Xu H et al (2018) CTAB-PEG DNA extraction from fungi with high contents of polysaccharides. Mol. Biol.$^{+}$ 52(2018): 621-628
15. Jordan DB, Bowman MJ, Braker JD et al (2012) Plant cell walls to ethanol. Biochem. J. 442(2): 241-252

16. Kanwal HK, Reddy MS (2012) The effect of carbon and nitrogen sources on the formation of sclerotia in *Morchella* spp. Ann Microbial. 62(2012): 165-168
17. Krastanova I, Guarnaccia C, Zahariev S et al (2005) Heterologous expression, purification, crystallization, X-ray analysis and phasing of the acetyl xylan esterase from *Bacillus pumilus*. BBA-Proteins Proteom. 1748(2): 222-230
18. Krishna G, Samatha B, Hima BS et al (2015) Macrofungi in some forests of Telangana State, India. J. Mycol. 2015(10): 1- 7
19. Liu X, Wang X, Kang K et al (2022) Review on extraction, characteristic, and engineering of the *Eucommia ulmodies* rubber for industrial application. Ind. Crop. Prod. 180(10): 1147-1161
20. Mckelvey SM, Murphy RA (2017) Biotechnological use of fungal enzymes. Fungi: Biology and Applications (Kavanagh K, Third Edition). Wiley Backwell, Britain, pp 201-225
21. Meng QS, Zhang F, Liu CG et al (2021) Measurement of cellulase and xylanase activities in *Trichoderma reesei*. Methods in Mol. Biol. (Clifton, N.J.) pp: 135-146
22. Mešić A, Šamec D, Jadan M et al (2020) Integrated morphological with molecular identification and bioactive compounds of 23 Croatian wild mushrooms samples. Food Biosci. 17(37): 100-113
23. Passari AK, Mishra VK, Leo VV et al(2016) Antimicrobial potential, identification and phylogenetic affiliation of wild mushrooms from two sub-tropical semi-evergreen Indian forest ecosystems. PLoS One. 11(30): 1-24
24. Qian SY, Zhang C, Zhu Z et al (2020) White rot fungus *Inonotus obliquus* pretreatment to improve trans-1, 4-polyisoprene extraction and enzymatic saccharification of *Eucommia ulmoides* leaves. Appl. Biochem. Biotech. 192(2020): 719-733
25. Roy DR, Krishnappa M (2018) Mycochemical profiling of *Lentinus squarrosulus* Mont., a wild edible macrofungi using GC-MS. IJPSR 9(10): 4349-4354
26. Senanayake IC, Rathnayaka AR, Marasinghe DS et al (2020) Morphological approaches in studying fungi: collection, examination, isolation, sporulation and preservation. Mycosphere. 11(1): 2678-2754
27. Shawn PB, Anne RR, Jumpponen A (2014) Analyses of ITS and LSU gene regions provide congruent results on fungal community responses. Fungal Ecol. 9(2014): 65-68
28. She D, Dong J, Zhang JH et al (2019) Development of black and biodegradable biochar/gutta percha composite films with high stretchability and barrier properties. Compos Sci. Technol. 175(3): 1-5
29. Shi Q, He Y, Zhang X et al (2022) Extraction of high-purity native state gutta-percha from enzymatic hydrolyzed *Eucommia ulmoides* pericarps by ultrasound treatment and surfactant aqueous phase dispersion. Agriculture. 12(7): 904-912
30. Sipos B, Benkő Z, Dienes D et al (2010) Characterisation of specific activities and hydrolytic properties of cell-wall-degrading enzymes produced by *Trichoderma reesei* Rut C30 on different carbon sources. Appl. Biochem. Biotech. 161(7): 347-364
31. Sista AK, Qin W (2018) Understanding the structural and functional properties of carbohydrate esterases with a special focus on hemicellulose deacetylating acetyl xylan

esterases. Mycology. 9(4): 273-295

32. Soccol CR, Da CF, Letti LJ et al (2017) Recent developments and innovations in solid state fermentation. Biotech. Res. and Innov. 1(1): 52-71
33. Song L, Xing X, Guo S (2018) Morphological process and regulation mechanisms of fruiting body differentiation in macrofungi: A review. Mycosystema. 37(11): 671-684
34. Sridhar KR, Deshmukh SK (2019) The macrofungal resource. advances in macrofungi: diversity, ecology and biotechnology. CRC, India, pp 1-9
35. Terrett OM, Dupree P (2019) Covalent interactions between lignin and hemicelluloses in plant secondary cell walls. Curr. Opin. Biotech. 56(2019): 97-104
36. Tuo Y, Rong N, Hu J (2022) Exploring the relationships between macrofungi diversity and major environmental factors in Wunvfeng National Forest Park in Northeast China. J. Fungi 8(2): 98-112
37. Undan JQ, Alfonso DO, Dulay RM (2016) Molecular identification and phylogeny of different macrofungi in Mt. Bangkay, Cuyapo, Nueva Ecija, Philippines based on ITS nrDNA region. Adv. in Environ. Bio. 10(12): 35-43
38. Wang Q, Xiong Y, Dong F (2021) *Eucommia ulmoides* gum-based engineering materials: fascinating platforms for advanced applications. J. Mater. Sci. 56(2021): 1855-1878
39. Wei XN, Peng P, Feng P et al (2021) Natural polymer *Eucommia ulmoides* rubber: a novel material. J. Agr. Food Chem. 69(13): 3797-3821
40. Wu DM (2015) Molecular phylogentics and genetic diversity of *Morchella* in Xinjiang. *China Agriculture University*, Beijing, pp: 1-87
41. Wu M, Liu P, Wang S et al (2021) Ultrasonic Microwave-assisted micelle combined with fungal pretreatment of *Eucommia ulmoides* leaves significantly improved the extraction efficiency of total flavonoids and gutta-percha. Foods 10(10): 2399-2415
42. Xie YF. Qin LJ, Zhao DG (2023) Preparation of gutta-percha through fermentative degradation of *Eucommia ulmoides* Oliver leaves by recombinant yeast expressing cellulases from *Trichoderma reesei*. Ind. Crop Prod 192(2023): 115830
43. Xu LL, Liang JD, Cai YH et al (2018) Optimization of process parameters under solid state fermentation using Eucommiae cortex as medicinal substrate by *Cordyceps militaris* (L.) Link. Guangdong Agr. Sci. 45(8): 83-90
44. Yan B, Tao Y, Huang C et al (2022) Using one-pot fermentation technology to prepare enzyme cocktail to sustainably produce low molecular weight galactomannans from *Sesbania cannabina* seeds. Appl. Biochem. Biotech 194(2022): 16-30
45. Yang H, Zhang H, Wang C et al (2019) Simple process to produce high-yield cellulose nanocrystals using recyclable citric/hydrochloric acids. ACS Sustainable Chem. Eng 7(5): 4912-4923
46. Yuan T, Qin LJ, Zhao DG (2021) Effects of different extraction methods on extraction yield and properties of *Eucommia* rubber. J. Central South University of Forest Tech. 41(7): 175-181

47. Zeng Q, Wei CB, Xia F (2018) Optimization of ultrasonic-assisted extraction of *Eucommia ulmoides* leaves Fu brick tea chlorogenic acid via response surface analysis and its hypoglycemic and antioxidant activities in vitro. Food and Fermentation Ind 44(18): 204-211
48. Zhang ZL, Yao ZL, Yan W (2015) Molecular identification of the isolates of *Tricholoma mongolicum*. Biotechnol. 21(5): 40-43
49. Zhou D, Dong G, Li FH et al (2021) Purification and comparative study of bioactivities of a natural selenized polysaccharide from *Ganoderma Lucidum* mycelia. Int. J. Biol. Macromol 190(1): 101-112
50. Zhou FL (2009) China · Guizhou higher fungi primary color map. Guizhou Science and Technology Press, Guiyang, pp 1-241.
51. Zhou P, PengZ (2018) Extraction of *Eucommia ulmoides* gum from *Eucommia ulmoides* fruit shell pretreated by acetic acid. Chinese J. Bioproc. Eng 16(3): 61-64
52. Zhu MQ, Sun RC (2018) *Eucommia ulmoides* Oliver: A potential feedstock for bioactive products. *J. Agr.* Food Chem 66(22): 5433-5438
53. Singh S, Tyagi CH, Dutt D et al (2018) Production of high level of cellulase-poor xylanases by wild strains of white-rot fungus Coprinellus disseminatus in solid-state fermentation. New Biotechnol 26(3&4): 165-170
54. Singh S, Dutt D, Tyagi CH et al (2011) Bio-conventional bleaching of wheat straw soda–AQ pulp with crude xylanases from SH-1 NTCC-1163 and SH-2 NTCC-1164 strains of Coprinellus disseminatus to mitigate AOX generation. New Biotechnology 28(1) 47-57

Tables

Table 1 Primer sequences for PCR amplification

Conserved sequences	Primer	Sequences（5’→3’）
ITS	ITS1	TCCGTAGGTGAACCTGCGG
	ITS4	TCCTCCGCTTATTGATATGC
LSU	LROR	ACCCGCTGAACTTAAGC
	LR5	TCCTGAGGGAAACTTCG

Table 2. Yields of cEUG/rEUG from fermented leaves with BJ-1 cultured with different conditions (mean±SE)

		7 d		14 d	
	Culture conditions	cEUG yield/%	rEUG yield/%	cEUG yield/%	rEUG yield/%
1	Medium - free	23.816±0.308e	1.624±0.022c	24.955±0.342c	1.606±0.049d
2	Medium - free + BJ-1	26.508±1.033d	1.679±0.029c	28.508±0.730bc	1.714±0.011c
3	Carbon -free + BJ-1	29.563±1.539c	1.830±0.036b	25.041±1.069c	1.609±0.009d
4	Xyl-carbon medium + BJ-1	51.623±9.861a	2.156±0.031a	49.728±3.912a	2.142±0.044a

Note: n=3. Lowercase letters represent for significant differences at P <0.05, cEUG represented for crude *E. ulmoides* gum, while rEUG represented for refined *E. ulmoides* gum.

Figures

Figure 1

Investigation of ecological environment and observation of fruiting body in genus *Coprinellus*

A, Ecological environment; B, Fruiting body (macro Lens); C, Fruiting body (lateral plan); D, Fruiting body (top view); E, Numbering

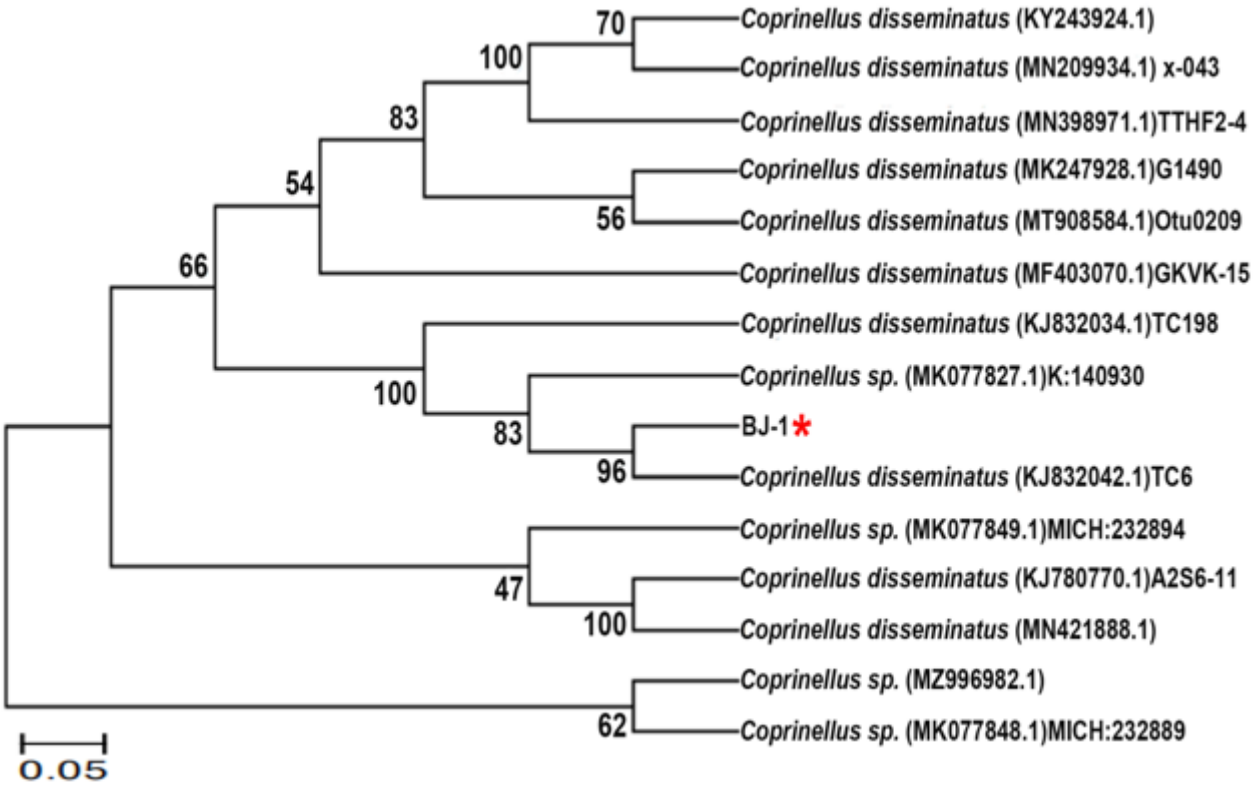

Figure 2

Phylogenetic tree construction of BJ-1 strain and related species based on ITS sequence

Note: Red star represented for collecting macrofungi

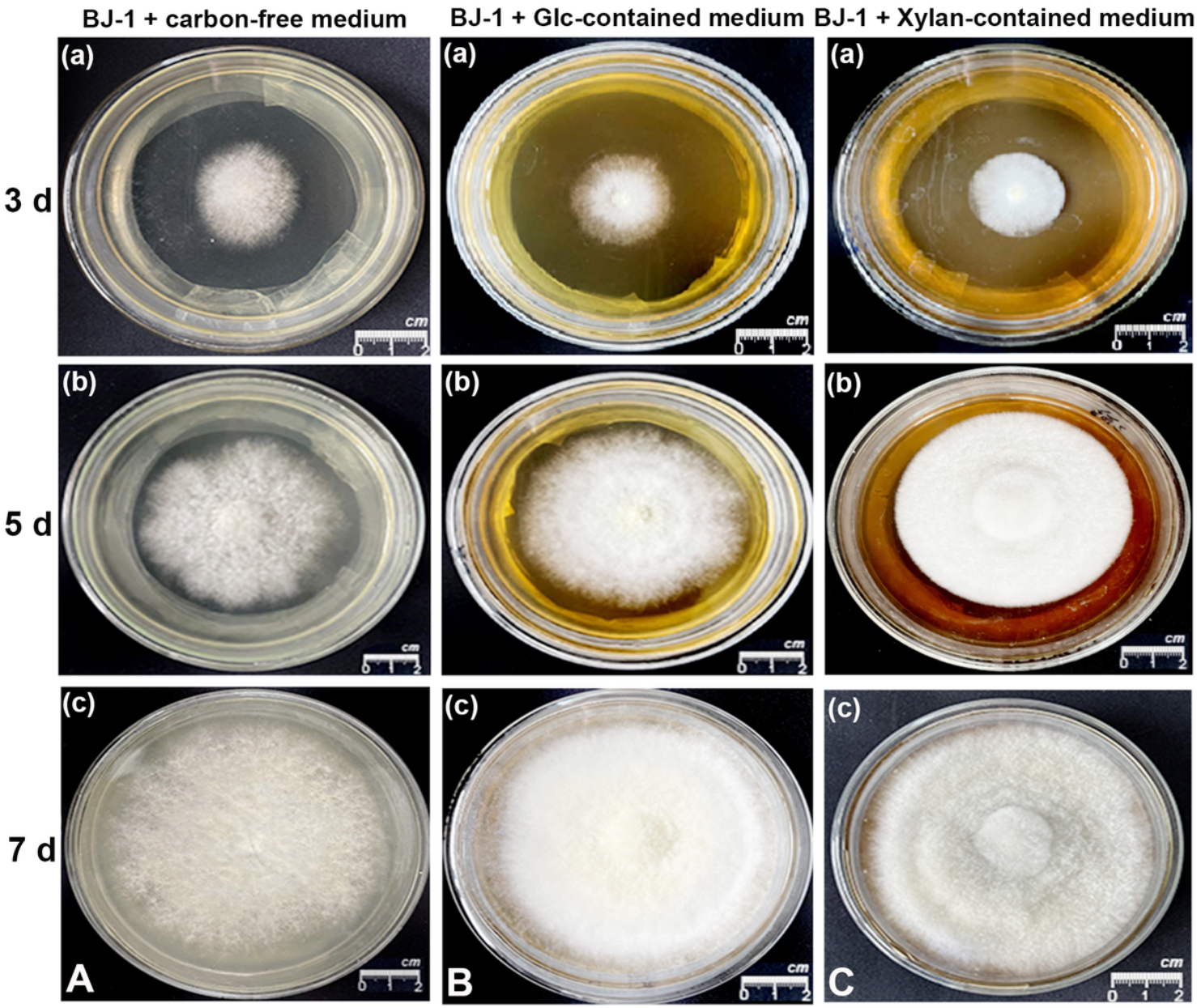

Figure 3

Effects of medium with different carbon sources on mycelium morphology in BJ-1

Note: A represented for growth situation of BJ-1 on carbon-free medium at different days; B represented for growth situation of BJ-1 on Glc-contained medium at different days; C represented for growth situation of BJ-1 on xylan-contained medium at different days

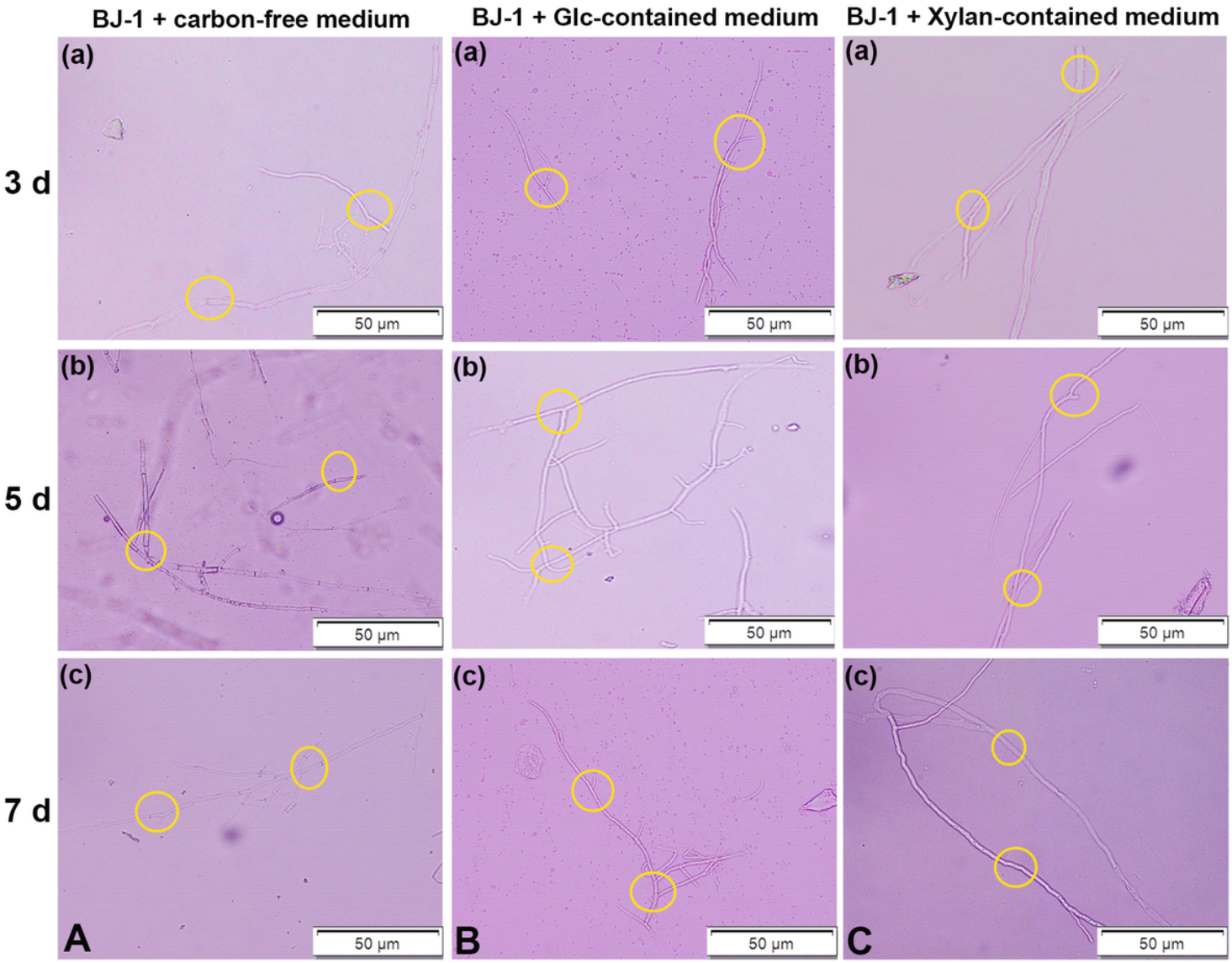

Figure 4

Effects of medium with different carbon sources on BJ-1 hypha

Note: A, B and C represented for the same meaning above

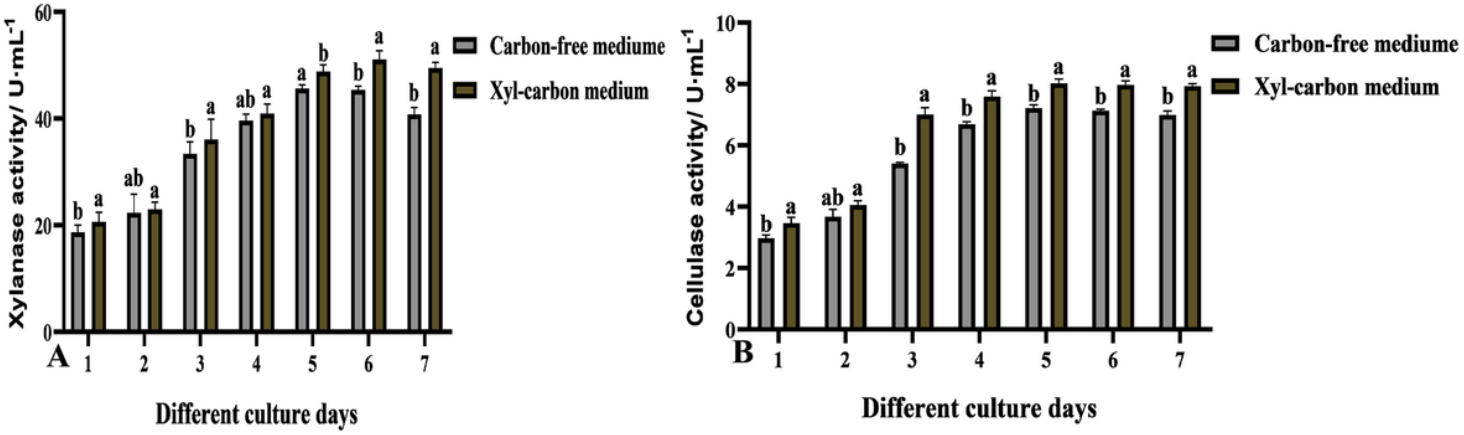

Figure 5

Effects of different culture conditions on cellulose and xylanase activity of BJ-1

Note: A represented for the changes in xylanase activity; B represented for the changes in cellulose activity

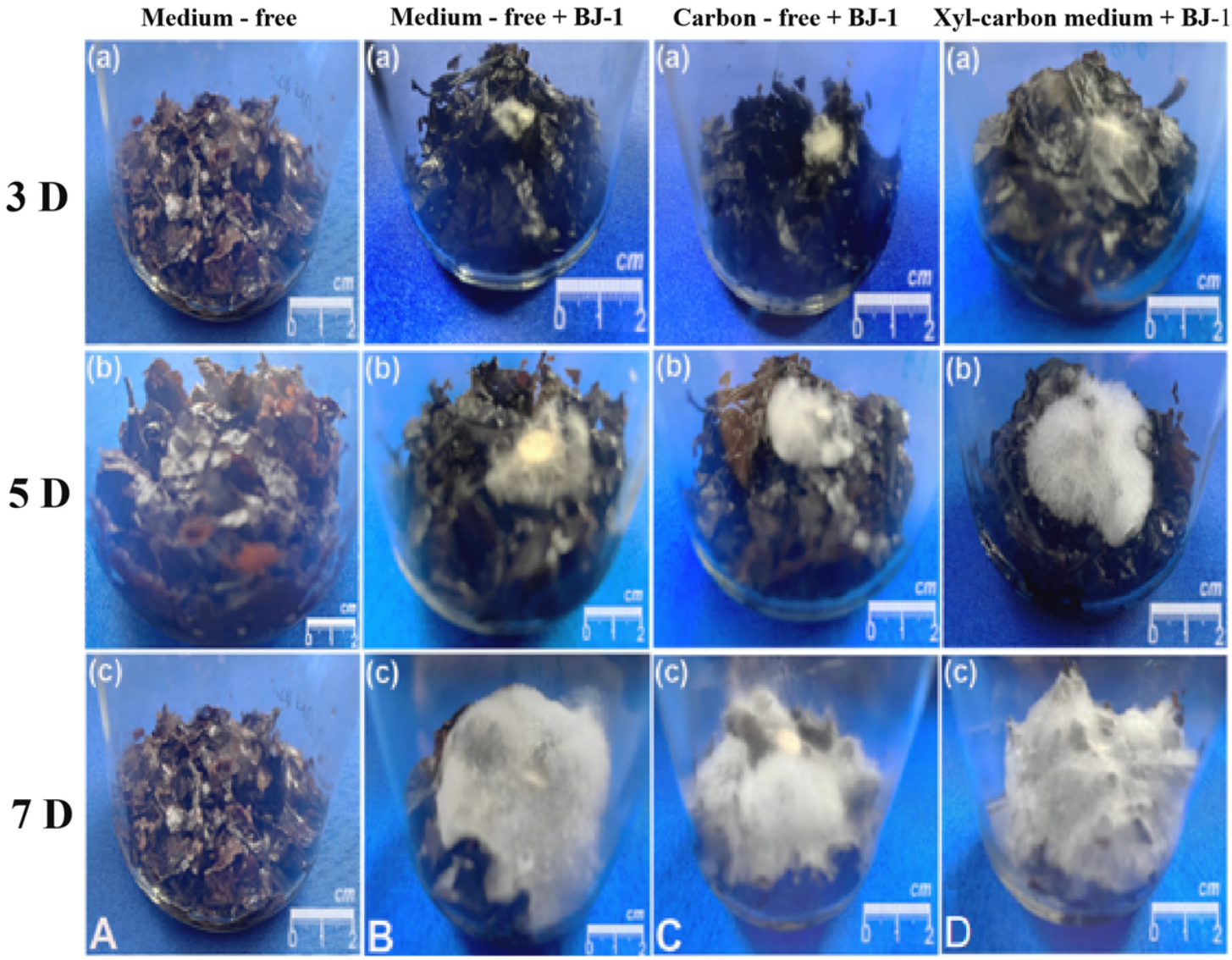

Figure 6

Effects of *E. ulmoides* leaves supplemented with different medium on BJ-1 mycelium growth

Note: A represented for sterile water only; B represented for sterile water with BJ-1; C represented for liquid carbon-free medium with BJ-1; D represented for liquid xylan-contained medium with BJ-1

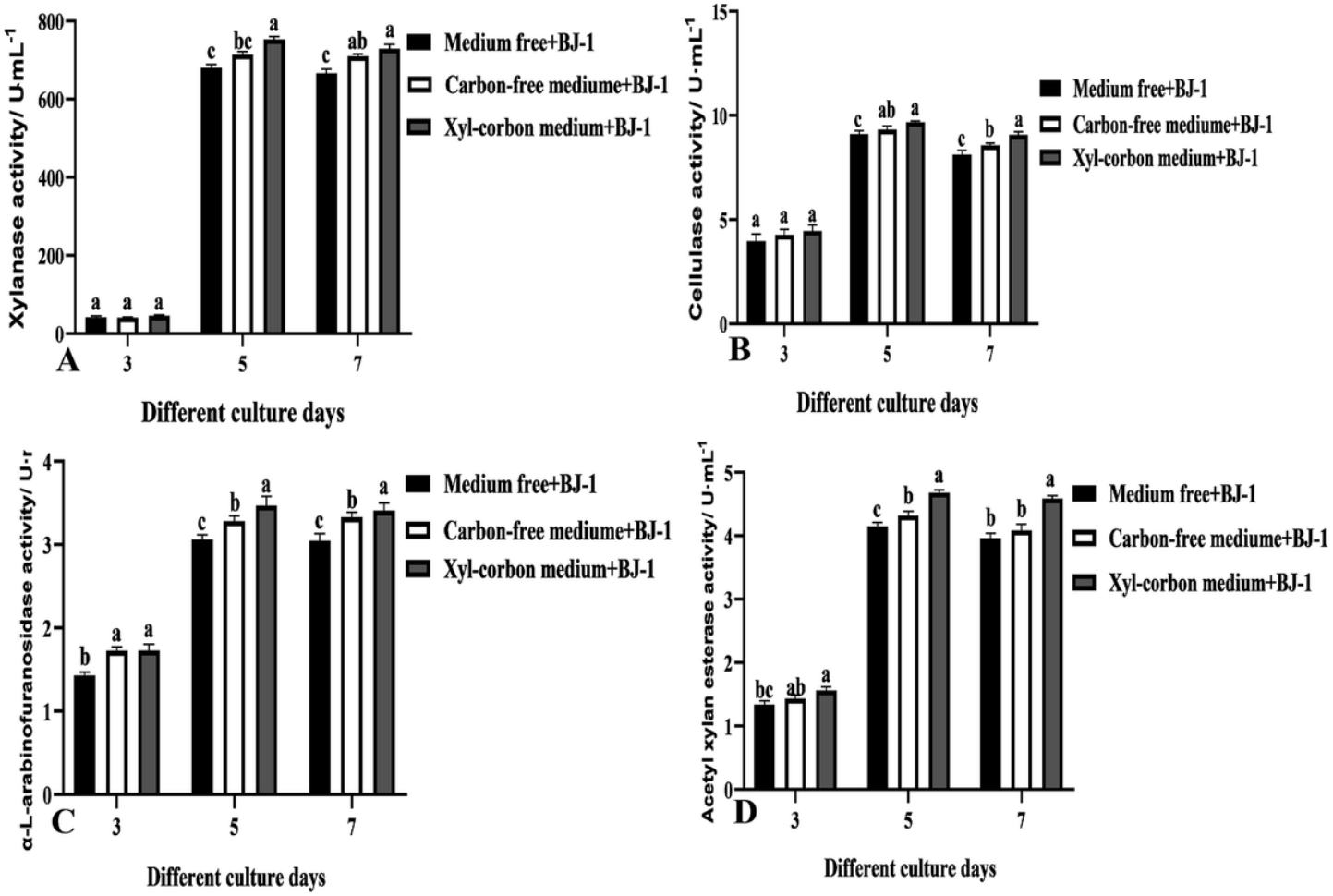

Figure 7

Effects of different with different culture conditions on cellulose degradation-related enzyme activities of BJ-1

Note: A represented for the changes in xylanase activity; B represented for the changes in cellulose activity; C represented for the changes in acetyl xylan esterase activity; D represented for the changes in α-L-arabinofuranosidase activity

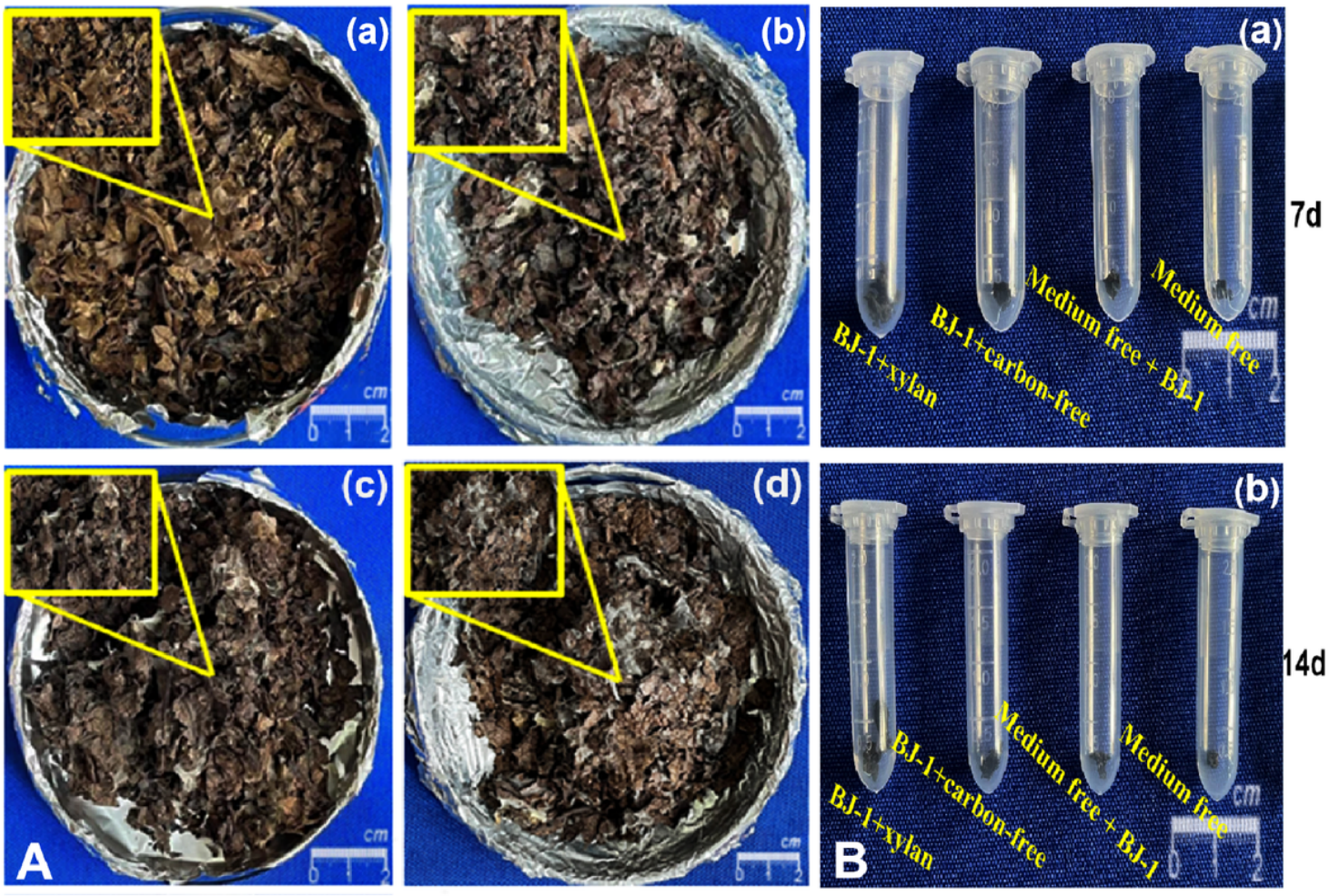

Figure 8

Morphological comparison of *E. ulmoides* leaves under different fermentation conditions and extraction of refined *E. ulmoides* gum

Note: Aa represented for the leaf fermentation added xylan-contained medium with BJ-1.Ab represented for the leaf fermentation added sterile water only; Ac represented for the leaf fermentation added sterile water with BJ-1; Ad represented for the leaf fermentation added carbon-free medium with BJ-1;

Supplementary Files

This is a list of supplementary files associated with this preprint. Click to download.

- Supplementarymaterials.doc